

Observations of the X-ray Nova GRO J0422+32:
II: Optical Spectra Approaching Quiescence.¹

Michael R. Garcia

Paul J. Callanan

Jeffrey E. McClintock

Ping Zhao

Center for Astrophysics, 60 Garden Street, Cambridge, MA 02138
E-mail: mgarcia,pcallanan,jmccclintock,pzhao, @cfa.harvard.edu

Submitted to ApJ: 1995 May 10, Revised 1995 August 31;

Subject Headings: accretion disks, stars:individual(GRO J0422+32)

¹Data reported herein was obtained with the Whipple Observatory MMT, an instrument jointly operated by the Smithsonian Astrophysical Observatory and the University of Arizona.

Observations of the X-ray Nova GRO J0422+32: II: Optical Spectra Approaching Quiescence.¹

Michael R. Garcia

Paul J. Callanan

Jeffrey E. McClintock

Ping Zhao

Center for Astrophysics, 60 Garden Street, Cambridge, MA 02138

E-mail: mgarcia,pcallanan,jmclintock,pzhao, @cfa.harvard.edu

ABSTRACT

We present results obtained from a series of 5 Å resolution spectra of the X-ray Nova GRO J0422+32 obtained in 1993 October, when the system was approximately 2 magnitudes above quiescence, with $R \sim 19$. The data were obtained in an effort to measure the orbital radial velocity curve of the secondary, but detection of the narrow photospheric absorption lines needed to do this proved elusive. Instead we found wide absorption bands reminiscent of M star photospheric features. The parameters determined by fitting accretion disk line profiles (Smak profiles) to the $H\alpha$ line are similar to those found in several strong black-hole candidates. Measurements of the velocity of the $H\alpha$ line are consistent with an orbital period of 5.1 hours and a velocity semi-amplitude of the primary of $34 \pm 6 \text{ km s}^{-1}$. These measurements, when combined with measurements of the velocity semi-amplitude of the secondary made by others, indicate that the mass ratio $q \sim 0.09$. If the secondary follows the empirical mass-radius relation found for CVs, the low q implies a primary mass of $M_x \sim 5.6M_\odot$, and a rather low (face-on) inclination.

¹Data reported herein was obtained with the Whipple Observatory MMT, an instrument jointly operated by the Smithsonian Astrophysical Observatory and the University of Arizona.

The $H\alpha$ EW is found to be modulated on the orbital period with a phasing that implies a partial eclipse of the disk by the secondary, but simultaneous R band photometry shows no evidence for such an eclipse.

1. Introduction

Low Mass X-ray Binaries (LMXBs) are systems where a neutron star or black hole accretes material from a low mass ($M \leq 1M_{\odot}$) secondary (see Bhattacharya and van den Heuvel 1991). X-ray novae (XRN) form a subset of LMXBs whose properties are characterized by dramatic increases in flux (factors of $\sim 10^5$ – 10^7) at X-ray and radio energies on time scales of days, with a subsequent decay to quiescence on time scales of months.

While these transients are in outburst, their X-ray and optical properties are very similar to those of the persistently bright LMXBs, where the optical flux is dominated by the reprocessed emission from the X-ray irradiated disk. In quiescence, however, the disk often fades to reveal the secondary star itself. This allows detailed photometric and spectroscopic measurements of the secondary to be made – otherwise impossible in the outburst state, and in most of the persistently bright LMXBs.

Studies of quiescent XRN are especially important for the following reasons. The frequency of black hole candidates among X-ray novae appears to be remarkably high; 9 out of the 13 optically identified systems are strong or probable black hole candidates (van Paradijs and McClintock 1995). Our understanding of the evolution of LMXBs (eg, the progenitors, lifetimes, and numbers) will be limited until we understand the nature of the transient sources. This is because the number of “dormant” transients may well exceed the number of persistent LMXBs by one to two orders of magnitude (van den

Heuvel 1992).

The detection of the photospheric lines of the secondary in quiescent systems allows measurement of the orbital radial velocity curve, leading to firm lower limits on the mass of the accreting object. These measurements indicate masses $\gtrsim 3M_{\odot}$ for the X-ray nova A0620-00 (McClintock and Remillard 1986), V404 Cyg (Casares, Charles and Naylor 1992) Nova Muscae 1991 (Remillard, McClintock and Bailyn 1992), Nova Ophiuci 1977 (Remillard *et al.* 1995), GRO J1655-40 (Bailyn *et al.* 1995), and GS2000+25 (Casares, Charles and Marsh 1995). Because the maximum mass for a stable neutron star is $\sim 3M_{\odot}$ (Chitre and Hartle 1976) these six XRN are regarded as strong black hole candidates. The mass ratio q can be determined by combining the measurements of the orbital velocity of the secondary with similar measurements of emission lines originating in the accretion disk. Models for formation of emission lines in accretion disks depend on many parameters, among them the inclination, inner and outer disk radii, and central object mass, and comparison to observed profiles can help to constrain some of these parameters.

In Callanan *et al.* 1995 (Paper I) we discussed the discovery of GRO J0422+32, and presented the first results from our optical observing campaign during the outburst and decline. In this paper we present the results of extensive spectroscopic observations obtained ~ 430 days after outburst, when GRO J0422+32 had decayed to $R \sim 19$ (see Figure 1). Our continuing photometric observations show that the source subsequently reached its quiescent level at day ~ 760 . The average intensity during days 760–950 is $R = 20.94 \pm 0.11$ (28 measurements) and $V = 22.35 \pm 0.17$ (3 measurements). We note that the error on the R magnitude in quiescence quoted here is computed from the observed scatter in the data, and may be dominated by intrinsic variability in the source. The outburst amplitude was $\Delta V \sim 9.0$, which is the largest yet seen for an XRN: typical outburst amplitudes are $\Delta V = 5 - 7$ magnitudes (van Paradijs and McClintock 1995).

2. Observations

By 1993 October 10, ~ 14 months after the initial outburst, GRO J0422+32 had reached $R \sim 19$ (day 430 on Figure 1), but was still at least ~ 2 magnitudes brighter than its quiescent level. This is surprising given that the black hole candidates Nova Muscae 1991 (Remillard, McClintock and Bailyn 1992), GS2000+25 (Chevalier and Ilovaisky 1990), and V404 Cyg (Casares and Charles 1992) had reached quiescence within 14 months of the outburst.

Spectra of GRO J0422+32 were obtained with the SAO Whipple Observatory MMT Red Channel Spectrograph on 1993 October 10 and 12 (UT), and spectra of several bright standards were obtained on October 11 (UT) for use in determining absolute radial velocities and spectral types. The spectra were obtained with a Loral 1200×800 pixel CCD having 7 electrons read noise. The combination of the grating and $1''$ slit gave $\sim 5 \text{ \AA}$ FWHM spectral resolution and spectral coverage from $\sim 5000 \text{ \AA}$ through $\sim 6700 \text{ \AA}$. The seeing on October 10 and 12 was predominantly $\sim 1''$ and the skies were mostly clear, but occasional clouds and intervals of worse seeing ($\sim 2''$) compromised the photometric accuracy of our spectra. The cloud cover on October 11 was sufficiently heavy that only bright standards were visible on the TV guider; however GRO J0422+32 was easily visible on the other two nights. The slit was approximately maintained at the parallactic angle in order to maximize throughput. Twenty minute integrations of GRO J0422+32 were bracketed by short exposures of a HeArNe lamp for wavelength calibration purposes. Data were reduced and analyzed using standard IRAF routines. Sixteen spectra were obtained on each night for a total exposure time of 640 minutes on GRO J0422+32. Simultaneous Whipple Observatory 1.2 m R band photometry was obtained; the instrumentation and data reduction are described in Callanan *et al.* 1995.

3. Analysis and Results

3.1. Cross-Correlation Results

Our primary goals were to detect the expected photospheric absorption lines due to the presumed late-type companion, and to measure the Doppler shifts in those lines due to the expected orbital motion of the star. We attempted this by cross-correlating the 32 individual GRO J0422+32 spectra against the spectra of late-type dwarf templates, ranging from early K to mid M, which were obtained with the identical instrumental setup on Oct 11. Before cross-correlating, the regions around the 5577 Å and 5890 Å night-sky lines were replaced with a fit to the local continuum, because these night sky lines are strong enough to render subtraction in the individual 20 minute exposures problematic. In addition, the spectra were filtered in order to remove low-frequency features and in order to match the instrumental resolution of 5 Å. The low frequency filtering was achieved by subtraction of a 13th order cubic spline fit to the continuum, and removal of wavenumbers < 6 from the Fourier transform of the spectra (FT). This effectively removes all features on scales larger than $\sim 100\text{Å}$, including the instrumental response and possible TiO bands (see Section 3.2). The high frequency filter removed wavenumbers > 330 from the FT, which has the effect of smoothing the data on the intrinsic resolution of 5Å (~ 3.5 pixels per resolution element). In order to avoid the contaminating effects of the H-Balmer emission lines, only the region between 5000 Å and 6500 Å was used for the correlations.

We were not able to detect any narrow, late-type photospheric lines in this data set, despite extensive efforts. In order to quantify our lack of detection, we added various amounts of a late-type stellar spectrum (with NaD excised) to our individual GRO J0422+32 spectra, and computed cross-correlations. In keeping with the short period, we added dwarf (rather than giant) spectra. When a M3V spectrum accounts

for $\sim 10\%$, a M0V for $\sim 20\%$, or a K3V for $\sim 30\%$ of the total light, the correlations yield significant detections with R (Tonry and Davis 1979) values in excess of 3.0. In this way we estimate that the fractional contribution of any late-type stellar photosphere to the continuum light at $R \sim 19$ is less than $10\% \pm 5\%$, $20\% \pm 5\%$, or $30\% \pm 5\%$ for an assumed M3V, M0V or K3V companion, respectively.

3.2. Shape of the Continuum

Figure 2 shows the sum of the spectra obtained on October 10 (bottom) and October 12 (top). The most obvious features are double peaked $H\alpha$ emission and interstellar NaD 5890 \AA absorption. The NaD night sky line has not been excised because it is accurately subtracted in the summed spectrum, while the 5577 \AA has once again been removed. The NaD EW (1.2 \AA) is consistent with an interstellar origin. Less obvious in Figure 2 are troughs in the continuum with minima at $\sim 6200 \text{ \AA}$, $\sim 5900 \text{ \AA}$, and $\sim 5200 \text{ \AA}$. These troughs are more apparent in Figure 3, which shows a scaled plot of the October 10 GRO J0422+32 spectrum and a spectrum of a M3V star. The correspondence in the broad continuum features leads us to suspect that something like an M star photosphere is present in the spectra, even though cross-correlations show that the narrow lines expected from an M star are not detectable. We considered the possibility that these troughs might be an artifact of our data acquisition or reduction procedure; however, spectra of the nova V849 Oph ($R \sim 18$) which were taken on the same nights with the identical instrumental setup and reduced in the same way do not show these features. In addition, spectra taken by other observers a few months later also show evidence for bands indicative of a late-type stellar photosphere (Bonnet-Bidaud and Mouchet 1994), although the lower S/N and resolution of these spectra make the bands difficult to detect. The evidence for these bands was much weaker in our spectra

from October 12. This may be because the S/N in the October 12 data was slightly lower than on October 10 (see Figure 2), or it may be that the band strength is variable and the ~ 0.3 magnitude brightening on October 12 is related to their weaknesses. We therefore concentrate solely on the October 10 spectra for the remainder of this section.

We measured the EW of the strongest two features (at 5900\AA and 6200\AA) and compared them to the EW in the M3V star spectrum. We choose to compare to an M3V star because it is a good match to the spectral type of GRO J0422+32 determined in quiescence, which is $M2\pm 1V$ (Garcia *et al.* 1994, Filippenko *et al.* 1995). The continuum points and band limits are defined by the M3V star, and are 5805\AA - 6039\AA and 6145\AA - 6350\AA , as marked on Figure 3. The EW of these bands in GRO J0422+32 are $\sim 10\text{\AA}$, while they are $\sim 60\text{\AA}$ in the M3V star. Thus we see that $1/6$, or $\sim 17\%$ of the light may be due to an M3V star.

An independent estimate of the amount of apparent M star photosphere present in the spectra can be made by creating synthetic spectra consisting of the sum of an M3V star and an accretion disk, and looking for the best match to the GRO J0422+32 spectra. This method is sensitive to the slope of the continuum, whereas the previous method is sensitive only to the depth of the bands. We first de-reddened the GRO J0422+32 spectra for $A_V = 1.2$ (see Callanan *et al.* 1995), and then sum variable amounts of an M3V star and an $F_\lambda = F * \lambda^\alpha$ accretion disk spectrum. We choose a power law for the accretion disk spectrum because it is a sufficiently accurate representation of what has been seen in quiescent XRN. We measured the slope of the powerlaw from the published data on three XRN in quiescence. The results are shown in Table 1, along with the slope measured for GRO J0422+32 during the decay by Shrader *et al.* 1994. We then assumed the slope for GRO J0422+32 was equal to the mean of the values in Table 1, but in order to determine the errors below we allowed α to vary over the full range shown in the table.

We then searched for the minimum χ^2 between the observed and synthetic spectra w.r.t. the fraction (F) of accretion disk. The minimum χ^2 was not found to be unity, in part because the observed spectrum does not accurately match the narrow lines of the template M star. In order to estimate an error range for our fit, we re-scaled the error bars so that the best fit $\chi^2 = 1$ (see Shahbaz *et al.* 1994), and computed 68% confidence intervals at $\chi_{\min}^2 + 1$, (Avni 1976). In the best fit synthetic spectrum, the M3V star contributes between $20_{-14}^{+11}\%$ at 5000\AA and $50_{-28}^{+18}\%$ at 6500\AA , where the error ranges include the a contribution due to the range in slopes found in Table 1.

Given the rather substantial errors associated with measuring the contribution based on the slope of the continuum, we see that both measurements are consistent with the assumption that an M3V star photosphere contributed $\lesssim 20\%$ of the light in October 1993, when $R \sim 19$. This is marginally consistent with our lack of a result from the cross-correlations, as we would need $\sim 20\%$ of the light to be due to a late-type stellar photosphere in order to obtain reliable cross-correlation results.

3.3. $H\alpha$ profiles

The double peaked $H\alpha$ profiles shown in Figure 2 are similar to those seen in cataclysmic variables, where they are believed to arise because of Doppler shifts in an accretion disk around the compact object (Smak 1981, Horne & Marsh 1986). In order to test this hypothesis for GRO J0422+32 we have fit model profiles appropriate for optically thin, flat, Keplerian disks. The model and fitting methods are described in detail by Smak 1981 and Orosz *et al.* 1994. We restricted ourselves to models in which $\alpha = 1.5$ (α is the exponent of the radially dependent emission function), as this value is generally seen in dwarf nova disks in quiescence (Horne 1993), and has also been found in XRN disks in quiescence (Johnson, Kulkarni and Oke 1989, Orosz *et al.* 1994). If we use other values

for α the results of our model fits might be different (see Figure 4 of Johnson, Kulkarni and Oke 1989), but by restricting ourselves to $\alpha = 1.5$ we allow direct comparison to previous work, in particular Orosz *et al.* 1994.

As the steady state Smak model which we fit to the data predicts a symmetrical emission line profile, we begin by selecting 17 of our 32 spectra from October 10 and 12 such that the sum has red and blue peaks of equal amplitude. A sum of all 32 spectra produces a profile in which the blue peak dominates (Figure 2). This departure from symmetry might be explained by phase or time variable emission from an accretion disk hot spot seen in CVs and XRN (Johnson *et al.* 1989), or it might be due to poorly understood deviations from optically thin, Keplerian models which have previously been noted in XRN (Orosz *et al.* 1994, Haswell and Shafter 1990). We have not attempted to correct the average H α profile for the possible effects due to the motion of the compact primary or the H α absorption line expected from the secondary, as both of these effects are expected to be small in GRO J0422+32 and are typically ignored (ie, Johnson, Kulkarni and Oke 1989, Orosz *et al.* 1994). In any case, fits to the simple, symmetrical Smak models will allow comparison of the GRO J0422+32 line profile to those seen in other XRN and CVs (Orosz *et al.* 1994, Williams 1983.)

A first-order polynomial was fit to the 6350 Å – 6750 Å region (excluding H α) in order to subtract the continuum from the summed spectrum, and a chi-squared minimizing method was used to determine the best fit model parameters. The best fit parameters and 68% confidence intervals that we found are: $r_1 = 0.14 \pm 0.01$, $\lambda_0 = 6564.0 \pm 0.1$ Å, and $v_d = 442 \pm 10$ km s $^{-1}$, where r_1 is the ratio of the radii of the inner and outer edges of the H α emitting part of the disk, λ_0 is the central wavelength of the profile, and v_d is the velocity at the outer edge of the disk (which is very nearly equal to 1/2 the separation of the peaks, see Smak 1981). A comparison of the data and best fit profile can be seen in Figure 4.

3.4. H α Radial Velocity

Because the H α line forms in the accretion disk, one might expect that the line velocity reflects the motion of the compact object. Measurement of this velocity should then determine the orbital period and mass function, $f(m) = PK_x^3/2\pi G = (M_c \sin(i))^3 / (M_x + M_c)^2$, where P is the orbital period, K_x is the semi-amplitude of the orbital velocity variation of the primary (and of the H α line by our assumption), M_c is the mass of the companion, M_x the mass of the compact star, and i is the orbital inclination. The phase and mid-point (γ velocity) of the H α velocity curve relative to that of the secondary provide checks on the validity of the assumption. Studies of CVs (eg, Young, Schneider and Sackett 1981, Stover 1981) and XRN (Haswell and Shafter 1990 hereafter HS90, Orosz *et al.* 1994, Marsh, Robinson, and Wood 1994, hereafter MRW94) show that K_x determined from H α emission lines is indicative of the velocity of the primary, even though the phase and γ of the H α velocity curve are sometimes slightly offset from that expected.

However, the complex and variable shape of the H α line makes it difficult to measure a velocity that reliably traces the motion of the compact object. Several methods have been developed to help alleviate this problem, among them “double Gaussian fitting” (Schneider and Young 1980, Shafter 1983, Marsh *et al.* 1994) and Smak profile fitting (Orosz *et al.* 1994). We have employed a variant of these methods. A single Gaussian is fit to the outer (red and blue) portion of the H α line, excluding the central part of the line which can be affected by bright spot emission, optical depth effects, and other effects which may not reflect the motion of the compact object. In practice this outer portion is determined to be that portion in which the second derivative of the flux vs wavelength is > 0 as one approaches the line center. Because this is the section of the line in which the profile is steepest (the derivative is highest), its location is very sensitive to changes in the line velocity. We tested our method on data obtained for XRN Muscae 1991 by

Orosz and collaborators in February 1993, and we find values of K_x and T_0 (but not γ) that are consistent with those derived by the double Gaussian fitting and phase resolved Smak profile fitting methods (Orosz *et al.* 1994).

In order to improve the S/N and search for radial velocity variations the individual 20 minute GRO J0422+32 spectra were grouped into 6 equal phase bins (with 4-7 spectra in each bin) based on the suggested period of $P = 5.0944 \pm 0.0017$ hours, (Chevalier and Ilovaisky 1994b; we chose this period because it has the smallest error among the many consistent periods reported to date). For each profile a χ^2 minimizing method was used to determine the central wavelength, width, and amplitude of a fitted Gaussian and linear continuum model. The errors in the fitted parameters were determined by the rms to the fit. A sine curve with period fixed at 5.0944 hours was fitted to the velocities, which gave an amplitude $K_x = 34 \pm 6$ km s⁻¹ and $\gamma = 142 \pm 4$ (see Figure 5A). For comparison, Filippenko, Matheson and Ho (1995) find $K_x = 42 \pm 2$ km s⁻¹ and $\gamma = 26.0 \pm 1.6$ from recent observations in quiescence with the Keck telescope. We adopt the phase convention of Orosz *et al.* 1994 and Johnson *et al.* 1989, in which T_0 marks the closest approach of the compact object to the observer, and find $T_0 = \text{HJD } 2, 449, 270.978 \pm 0.004$.

3.5. H α EW and Continuum Variations

Previous studies of interacting binaries have shown that the relative phasing of variations in emission line velocities, emission line EW, and wide-band photometry has the potential to reveal much about the geometry of a binary system (eg, Pringle and Wade 1985, Mauche 1990). In order to measure the EW of the H α emission line, we fitted a low-order polynomial to the region around the emission line in each of the 32 spectra, in order to determine the continuum level. Figure 5B shows the resulting H α EW vs the phase we determined above. We find that the EW is modulated by a factor of ~ 2 on the orbital

period, varying between 20 Å and 40 Å. There is a broad minimum in the EW around phase 0.5.

We obtained 3 nights of R band photometry with the SAO 1.2 m telescope during October 1993. Two of these nights were simultaneous with the MMT spectra described herein, and are plotted vs phase in Figure 5C. These data are also shown in Callanan *et al.* 1995, Figure 3(d) [but note that they are labeled via MST dates, ie, October 9 and October 11]. The first seven measurements on October 12 are significantly (~ 0.2 magnitudes) higher than the rest, indicating a flare-like event from GRO J0422+32. We excluded these points from the analysis below. The solid line is the average magnitude in each of 12 phase bins. This average varies by 12%, and the mean rms in each of the 12 bins is 5%. There appears to be a broad maximum between phases 0.5 and 1.0, with a slight indication of a local maximum around phase 0.5.

4. Discussion

The apparently periodic modulation of the H α EW and velocity reported herein agree with the suggested ~ 5.1 hour orbital period for GRO J0422+32 (Chevalier and Ilovaisky 1994b), which has recently been confirmed by spectroscopic observations in quiescence (Orosz and Bailyn 1994, 1995; Filippenko *et al.* 1995, Casares *et al.* 1995).

The lack of a detection of the secondary from our cross-correlation efforts indicates that the secondary contributed only a small fraction of the light during October 1993. The fact that the system faded another 2 magnitudes since October 1993 by itself sets an upper limit of 16% to the contribution of the secondary in October 1993. The non-detection is consistent with tests of the sensitivity of the cross-correlations to detecting the secondary in the individual 20 minute spectra, which show that we would need a contribution of $\sim 20\%$ for reliable detection (Section 3.2). Somewhat surprisingly

the secondary does seem to be discernable in the grand sum spectrum, in that wide (but weak) M-star bands are seen in the spectrum. The measured strength of the bands may be somewhat larger than the 16% allowed contribution, however the errors in the measurement are large, and given the tendency to overestimate the strength of weak absorption features in noisy spectra it seems very likely that the bands are due to the M2V secondary.

The accretion disk parameters (and 1σ errors) derived using the Smak profile fits for GRO J0422+32 are compared to those derived for the XRN A0620-00 and X-ray Nova Muscae 1991 (Orosz *et al.* 1994) in Table 2. We see that the r_1 values derived for A0620-00 and GRO J0422+32 are very similar, and are a factor of two larger than that found for Nova Muscae. Interpreted in the context of the Smak model, this indicates that the ratio of the inner to outer radii of the H α emitting part of the disk is ~ 7 in A0620-00 and GRO J0422+32, but ~ 14 in Nova Muscae.

We can see in Figure 5 that the H α EW decreases by $\sim 50\%$ at phase 0.5, about the same time that the R band photometry increases by $\sim 12\%$. The relative amplitude of the EW and R band variations shows that only a small part of the the H α EW variations can be due to variations in the continuum. Casares *et al.* (1995) also find a $\sim 50\%$ orbital modulation in the H α EW of GRO J0422+32 in data taken in quiescence. This variation is in marked contrast to that seen in A0620-00 (MRW94) and V404 Cyg (Casares and Charles 1992, Casares *et al.* 1993), in which the H α EW modulation is largely explained by modulation in the underlying continuum. The H α velocities imply that the secondary is closest to the observer when the EW is smallest, which suggests that the EW variations may be due to an eclipse of the disk by the secondary. However, this is untenable for a simple azimuthally symmetric disk. The problem is that any eclipse would have to cover $\sim 50\%$ of the H α emitting region while at the same time the overall R band continuum (which must be due almost entirely to the disk) peaks. It is perhaps more likely that the EW variations are due to variations in the projected

geometry and integrated emissivity of the disk itself, for example due to an azimuthally varying disk thickness.

We searched for, and found, orbital radial velocity variations in the H α emission line. Such variations often measure the motion of the compact object in SXT (Orosz *et al.* 1994, HS90, MRW94). In the particular case of GRO J0422+32, we can check to see if this velocity variation is consistent with the compact object by comparing the γ velocity and phase to those measured for the secondary.

We find a central velocity of $\gamma = 142 \pm 4 \text{ km s}^{-1}$ for the H α line in GRO J0422+32, which is not consistent with velocity of the secondary of $\gamma = 10 \pm 4 \text{ km s}^{-1}$ (Filippenko *et al.* 1995). However, the γ velocities derived from SXT H α studies are somewhat problematic. The values derived depend strongly on the details of the function used to fit the line (ie, HS90, Orosz *et al.* 1994). It is therefore not surprising that different methods lead to different results. In the best studied system, A0620-00, Orosz *et al.* find $\gamma = 78 \pm 3$ via Smak profile fitting, but $\gamma = 1.5 \pm 0.8$ via double Gaussian fitting. Even when consistent methods are used, the H α γ in A0620-00 appears to change from year to year, perhaps because of variations in the shape of the H α profile (using double Gaussian fitting, HS90 find $\gamma = 28 \pm 6$ in Dec 89/Jan 90, Orosz *et al.* find $\gamma = 1.5 \pm 0.8$ in Jan 91/Feb 91, and MRW94 find $\gamma = 0 \pm 5$ in Dec 91/Jan 92). One is lead to the conclusion that H α γ velocities are not robust measures of the binary systemic velocity, and that in the case of GRO J0422+32 our measurement of $\gamma = 142 \pm 4 \text{ km s}^{-1}$ argues neither strongly for nor against the assumption that the H α velocity variations (K_x) are representative of the compact object. However, even given the problematic nature of the H α γ velocities, it appears that H α K_x velocities are accurate, in that they yield results which agree with those determined by independent methods (Orosz *et al.* 1994, MRW94).

The orbital period of GRO J0422+32 is not presently known with sufficient accuracy

to compare the phase of the secondary radial velocity curve measured in quiescence (Filippenko *et al.* 1995, Casares *et al.* 1995) to the H α curve we measured in October 1993. However, the large H α EW variations, seen once per orbital cycle, might provide an accurate fiducial mark. If one assumes this variation is stable with respect to the orbital phase, then we can use the EW curve to compare our H α velocities to those measured for the secondary. Comparing our Figure 5 A/B to Figure 1 of Casares *et al.* (1995), we see that the peak of the H α EW modulation occurs when the H α velocity crosses from blue to red, and the secondary velocity crosses from red to blue. This is the phasing expected if the H α velocities track the compact object.

By combining our measurement of the velocity semi-amplitude of the primary ($K_x = 34 \pm 6 \text{ km s}^{-1}$) with the recently determined velocity semi-amplitude of the secondary ($K_c = 380 \pm 6 \text{ km s}^{-1}$, Filippenko *et al.* 1995) we can determine the mass ratio $q = K_x/K_c = 0.089 \pm 0.016$. This mass ratio, while extreme, is similar to that found in other XRN and reinforces the idea that XRN as a class may have mass ratios extreme enough to excite SU UMa type superhumps in outburst (Callanan and Charles 1991, Bailyn 1992). Indeed, superhumps during outburst have been reported for GRO J0422+32 (Kato, Mineshige and Hirata 1995).

The mass function sets a lower limit to the mass of the compact object of $M_x = 1.21 \pm 0.04 M_\odot$ (Filippenko *et al.* 1995). When we use our estimate of the mass ratio (and the definition of the mass function) we find the lower limit is raised to $M_x > 1.43 \pm 0.09 \sin^{-3}(i) M_\odot$. The corresponding lower limit to the mass of the secondary is $M_c > 0.12 \pm 0.02 \sin^{-3}(i) M_\odot$.

A reasonable upper limit on the mass of the secondary might be derived from the empirical mass/period relation found for secondaries in CVs by Patterson (1984). We feel this is an upper limit because studies of Cen X-4, for example, show that the secondary in this X-ray binary is substantially undermassive (Remillard and McClintock 1990). For

the 5.1 hour period of GRO J0422+32, Patterson’s relation predicts $M_c = 0.5M_\odot$. Given the q found above, this translates into an upper limit for the mass of the compact object of $M_x < 5.6 \pm 1.4M_\odot$, and (through the mass function) a lower limit to the inclination of 35° . The lack of optical and x-ray eclipses sets an upper limit to the inclination of $i < 80^\circ$ at the observed mass ratio (Chanan, Middleditch, and Nelson 1976). The rather modest orbital modulation of the lightcurve compared to that seen in other XRN favors the lower end of the allowed range in i , and therefore the higher end of the allowed range in M_x . We note that the q and M_x we find are consistent with those determined from the observations of superhumps during outburst by Kato *et al.* (1995). However detailed modeling of the lightcurve (eg Haswell *et al.* 1993) will be necessary to further constrain i , q , and M_x .

We thank the staff at the MMTO for their outstanding level of support, and the multitude of observers at the WO 1.2 m telescope who helped collect the extensive light curve of GRO J0422+32. This work was partially supported by NASA contract NAS8-39073, grant NAGW-4296, and an Oxford University Visitors Grant. We thank Drs. Filippenko, Casares, and Orosz for providing results prior to publication, and we thank the referee for many helpful comments.

Table 1:

XRN	Wavelength Range	α	Reference
A0620-00	3000Å- 10000Å	-1.76	Oke 1977
XN Muscae 1991	5000Å- 6500Å	-1.88	Orosz <i>et al.</i> 1995
V404 Cyg	4400Å- 7000Å	-1.63	Casares <i>et al.</i> 1993
GRO J0422+32	4000Å- 7000Å	-1.80	Shrader <i>et al.</i> 1994

Table 2:

parameter	A0620-00	Nova Muscae	J0422+32
r_1	0.15 ± 0.01	0.07 ± 0.01	0.14 ± 0.01
v_d	550 ± 10	450 ± 10	442 ± 10

References

Avni, Y., 1976 ApJ 210 642

Bailyn, C.D., Orosz, J.A., McClintock, J.E., and Remillard, R.A., 1995, submitted to NATURE

Bailyn, C.D., 1992 ApJ 391, 298

Bonnet-Bidaud, J.M., and Mouchet, M., 1994, submitted to A&A

Callanan, P.J., Garcia, M.R., McClintock, J.E., Zhao, P., 1995 ApJ in press

Callanan, P.J., and Charles, P.A., 1991 MNRAS 249, 573

Casares, J. Charles, P.A., and Marsh, T., 1995, submitted to MNRAS.

Casares, J. *et al.*, 1995, accepted for publication in MNRAS

Casares, J. Charles, P.A., and Naylor, T., Pavlenko, E.P, 1993 MNRAS 265, 834

Casares, J. Charles, P.A., 1992 MNRAS 255, 7

Casares, J. Charles, P.A., and Naylor, T., 1992 NATURE 355, 614

Chanan, G.A., Middleditch, J., and Nelson, J.E., 1976 ApJ 208, 512

Chitre, D.M., and Hartle, J.B., 1976, ApJ 207, 592

Chevalier, C. and Ilovaisky, S.A., 1994b, IAUC 6118

Chevalier, C. and Ilovaisky, S.A., 1990 A&A 238, 163

Filippenko, A.V., Matheson, T., and Ho, L.C., 1995 ApJ, submitted

- Garcia, M.R., Callanan, P.J., McClintock, J.E., and Zhao, P., 1994 BAAS 25, 1381
- Haswell, C.A., Robinson, E.L., Horne, K., Stiening, R.F., and Abbott, T.M.C., 1993
Ap.J 411, 801
- Haswell, C.A., and Shafter, A.W., 1990 ApJ 359, L47
- Horne, K., 1993, Proceedings NATO ARW “Theory of Accretion Disks II, Munich,
Germany 22-25 March 1993
- Horne, K. and Marsh, T.R., 1986 MNRAS 218, 761
- Johnson, H.M., Kulkarni, S.R., and Oke, J.B. 1989, ApJ 345, 492
- Kato, T., Mineshige, S., Hirata, R., 1995, PASJ 47, 31.
- McClintock, J.E., and Remillard, R.A., 1986 ApJ 308, 110
- Marsh, T.R., Robinson, E.L., and Wood, J.H., 1994, MNRAS, 266, 137
- Mauche, C. W., 1990, Accretion Powered Compact Binaries, (Cambridge: Cambridge
University Press)
- Oke, J.B., 1977 ApJ 217, 181
- Orosz, J., and Bailyn, C., 1994, IAUC 6103
- Orosz, J.A., Bailyn, C.D., Remillard, R.A., McClintock, J.E., and Foltz, C.B., 1994, ApJ
436, 848
- Orosz, J.A., Bailyn, C.D., McClintock, J.E., and Remillard, R.A., 1995, ApJ (submitted)
- Orosz, J., and Bailyn, C., 1995, submitted to ApJ
- Patterson, J., 1984 ApJ Suppl 54, 443

- Pringle, J.E., and Wade, R.A., 1985, *Interacting Binary Stars*, (Cambridge, Cambridge University Press)
- Remillard, R.A., Orosz, J.A., McClintock, J.E., and Bailyn, C.D., 1995, *ApJ*, submitted
- Remillard, R.A., McClintock, J.E., and Bailyn, C.D., 1992 *ApJ* 399, L145
- Remillard, R.A., and McClintock, J.E., 1990 *ApJ* 350, 386
- Ritter, H., and Kolb, U., 1995, to appear in “X-ray binaries”, W.H.G. Lewin, J. van Paradijs, E.P.J. van den Heuvel (Eds.), Cambridge University Press (in press)
- Schneider, D.P. and Young P.J. 1980 *ApJ* 238, 946
- Shafter, A.W., 1983 *ApJ* 267, 222
- Shahbaz, T., Ringwald, F.A., Bunn, J.C., Naylor, T., Charles, P.A., and Casares, J. 1994 *MNRAS* 271, L10
- Shrader, C.R., Wagner, R.M., Hjellming, R.M, Han, X.H., and Starrfield, S.G., 1994 *ApJ* 434, 698
- Smak, J. 1981 *Acta Astr.* 31.4, 395
- Stover, R.J., 1981 *ApJ* 248, 684
- Tonry, J. and Davis, M. 1979 *AJ* 84, 1511
- Williams, G. 1983 *ApJ Suppl*, 53, 523
- Young, P., Schneider, D.P., and Sheckman, S.A., 1981 *ApJ* 245, 1035
- van Paradijs, J. and McClintock, J.E., 1995, to appear in “X-ray binaries”, W.H.G. Lewin, J. van Paradijs, E.P.J. van den Heuvel (Eds.), Cambridge University Press (in press)

van den Heuvel, E.P.J., 1992, Proc. Sat. Symp. Nr. 3, Int. Space Yr. Conf., Munchen,
(ESA ISY-3, July 1992), ESTEC, Noordwijk, p29

FIGURE CAPTIONS

Figure 1: The long term light curve of GRO J0422+32 in the R band, beginning a few days after discovery in 1992 August and continuing for more than two years. The spectroscopic observations reported here took place during days 430 and 432, in between the two mini-outbursts (at days ~ 370 and ~ 500) which were detected during the decay. The relative constancy of the data after day ~ 760 indicates that the system has now reached its quiescent magnitude of $R = 20.94 \pm 0.11$. An earlier version of this lightcurve appeared in Callanan *et al.* 1995.

Figure 2: The grand sum of the spectra obtained on 1993 October 10 (bottom) and October 12 (top). The y-axis is flux in units of $\text{ergs cm}^{-2}\text{sec}^{-1}\text{\AA}^{-1}$, with an offset of 0.2 added to the October 12 spectrum in order to clarify the plot. Simultaneous photometry from the 1.2 m telescope indicated that the mean brightness was slightly lower on October 10 and higher on October 12, with $R = 19.2$ and $R = 18.9$, respectively. The most prominent feature in the spectra is the double peaked $\text{H}\alpha$ emission line. These spectra have not been de-reddened. The EW of the NaD line (1.2\AA) is consistent with an interstellar origin.

Figure 3: Summed spectrum of GRO J0422+32 from 1993 October 10 compared to a M3V spectrum obtained as a cross-correlation template. The GRO J0422+32 spectrum has been de-reddened by $A_v = 1.2$. The straight lines indicate continuum points used to measure EW of absorption bands.

Figure 4: The summed $\text{H}\alpha$ profile of GRO J0422+32 and best fitting Smak model. The Smak model is appropriate for optically thin, Keplerian accretion disks.

Figure 5: Panel A shows the wavelength of the center of the H α emission line as observed at the telescope and as determined from Gaussian fits to the steepest section of the line, assuming a 5.0944 hour orbital period, plotted vs phase. The best fitting sine curve of $K_x = 34 \pm 6$ km s $^{-1}$ and heliocentric $\gamma = 142 \pm 4$ km s $^{-1}$ is superposed. The time of closest approach of the primary is $T_0 = \text{HJD}2,449,270.978 \pm 0.004$. Panel B shows the EW of H α vs the phase we have determined from the H α velocities. Panel C shows the R magnitudes from the SAO 1.2 m telescope, measured simultaneously with the H α EW. The circles are from October 10, the triangles from October 12, and the crosses are the “flare” data (see text) from the beginning of October 12 offset by 0.2 magnitudes. The solid line is the mean flux in each of 12 phase bins, and single error bar of 0.05 mag, representing the mean rms of the binned data, is shown.

Fig. 1.—

Fig. 2.—

Fig. 3.—

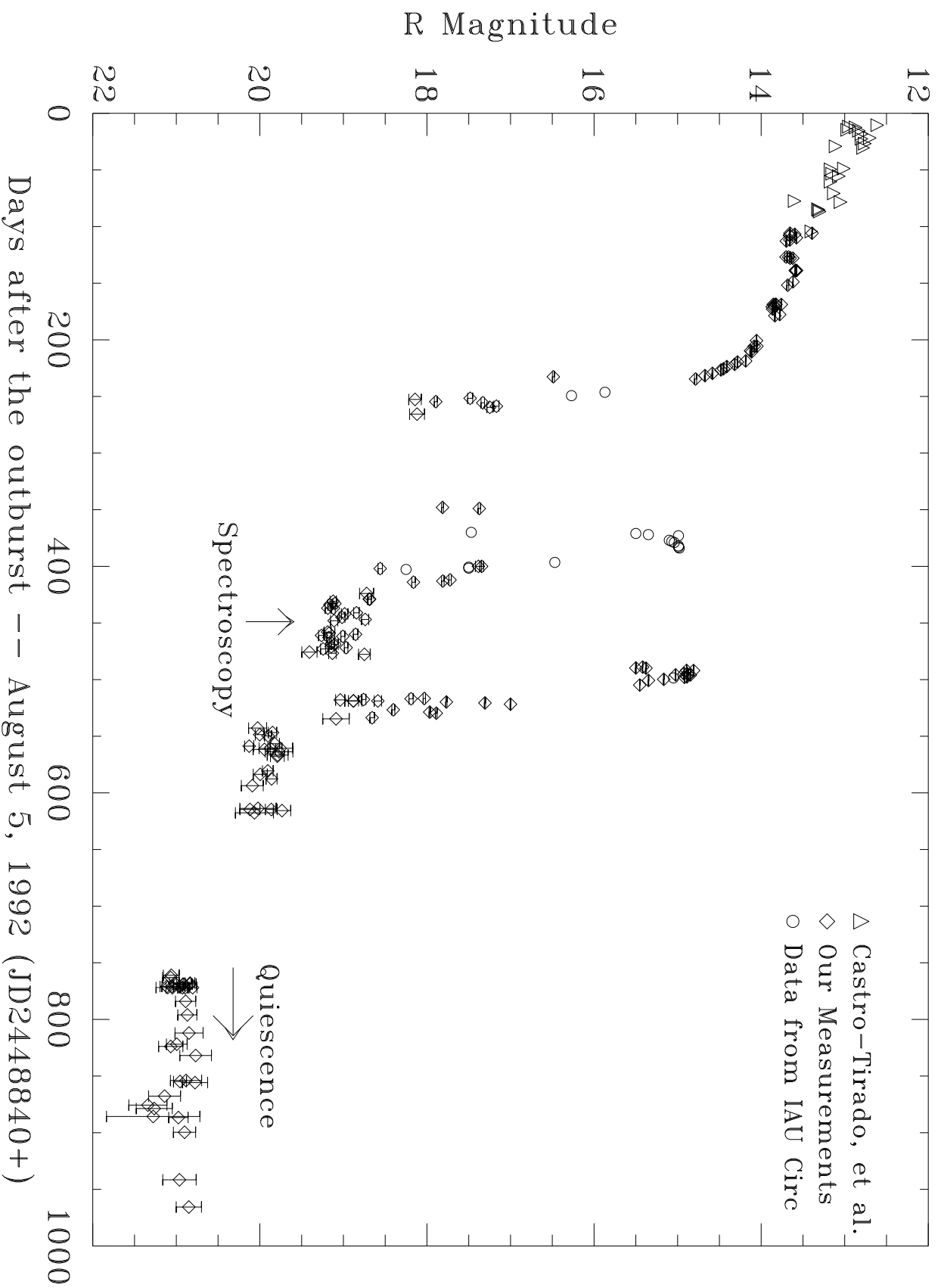
Fig. 4.—

Fig. 5.—

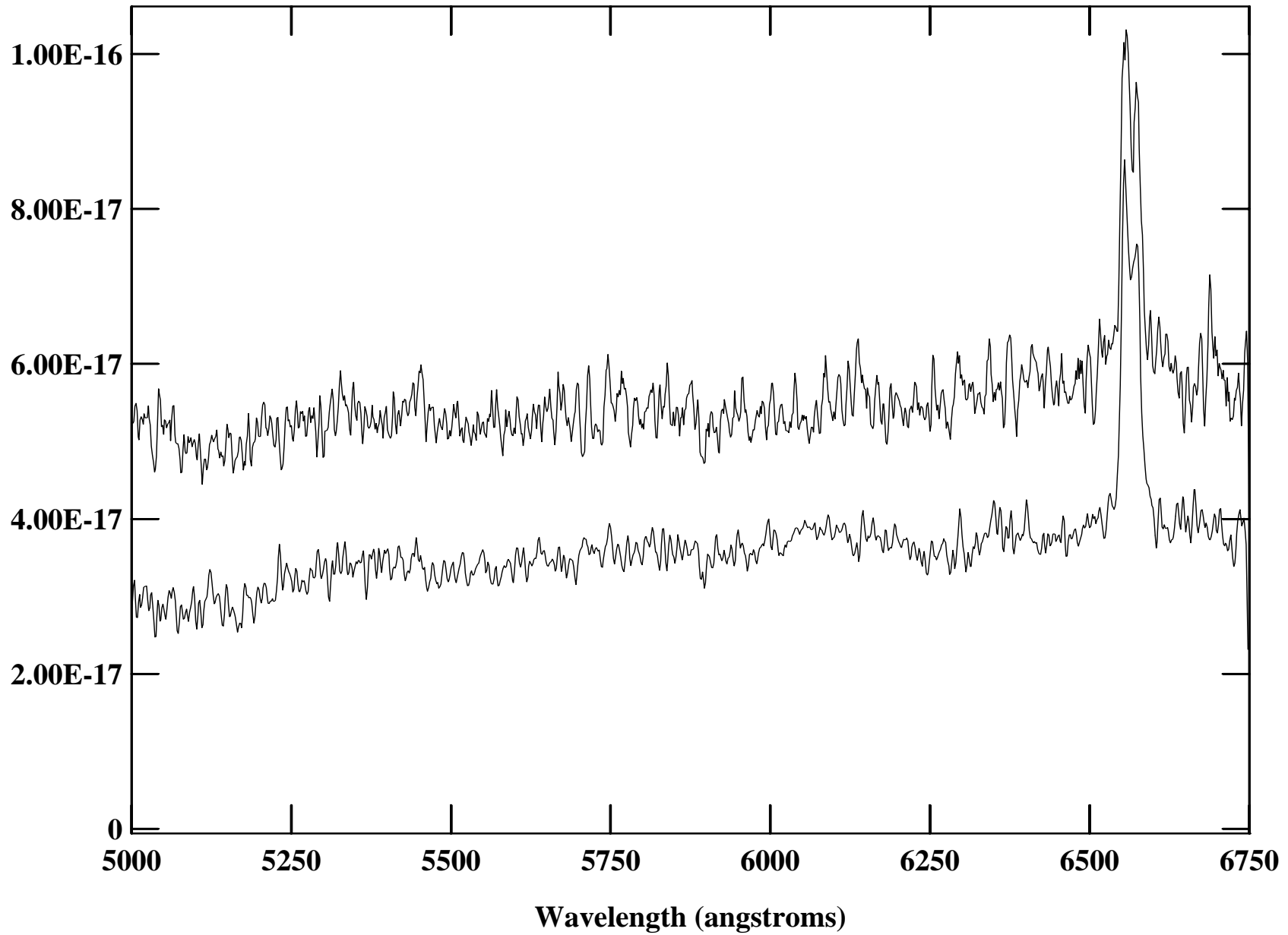
Fig. 6.—

Fig. 7.—

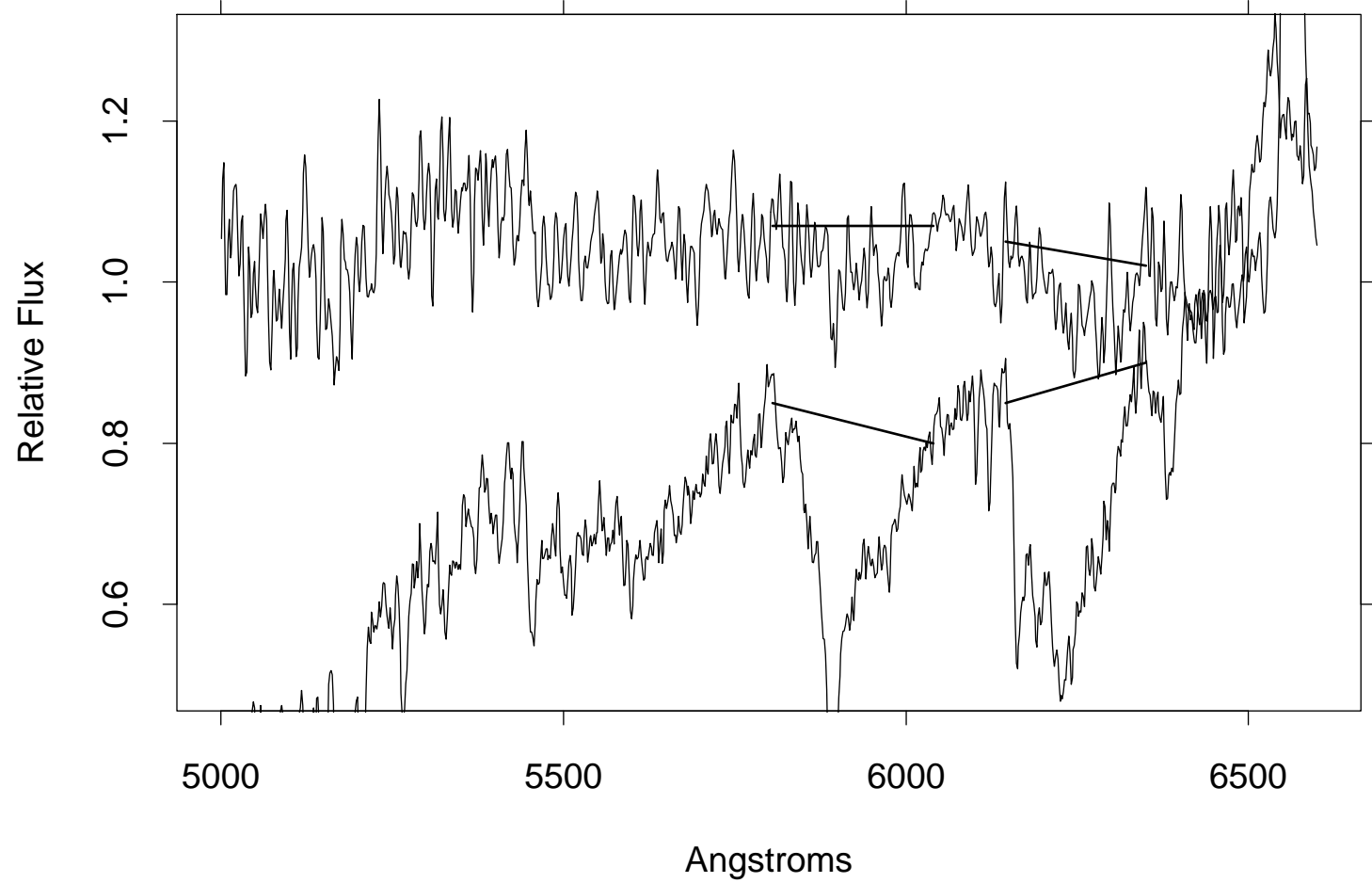
GRO J0422+32 Light Curve R



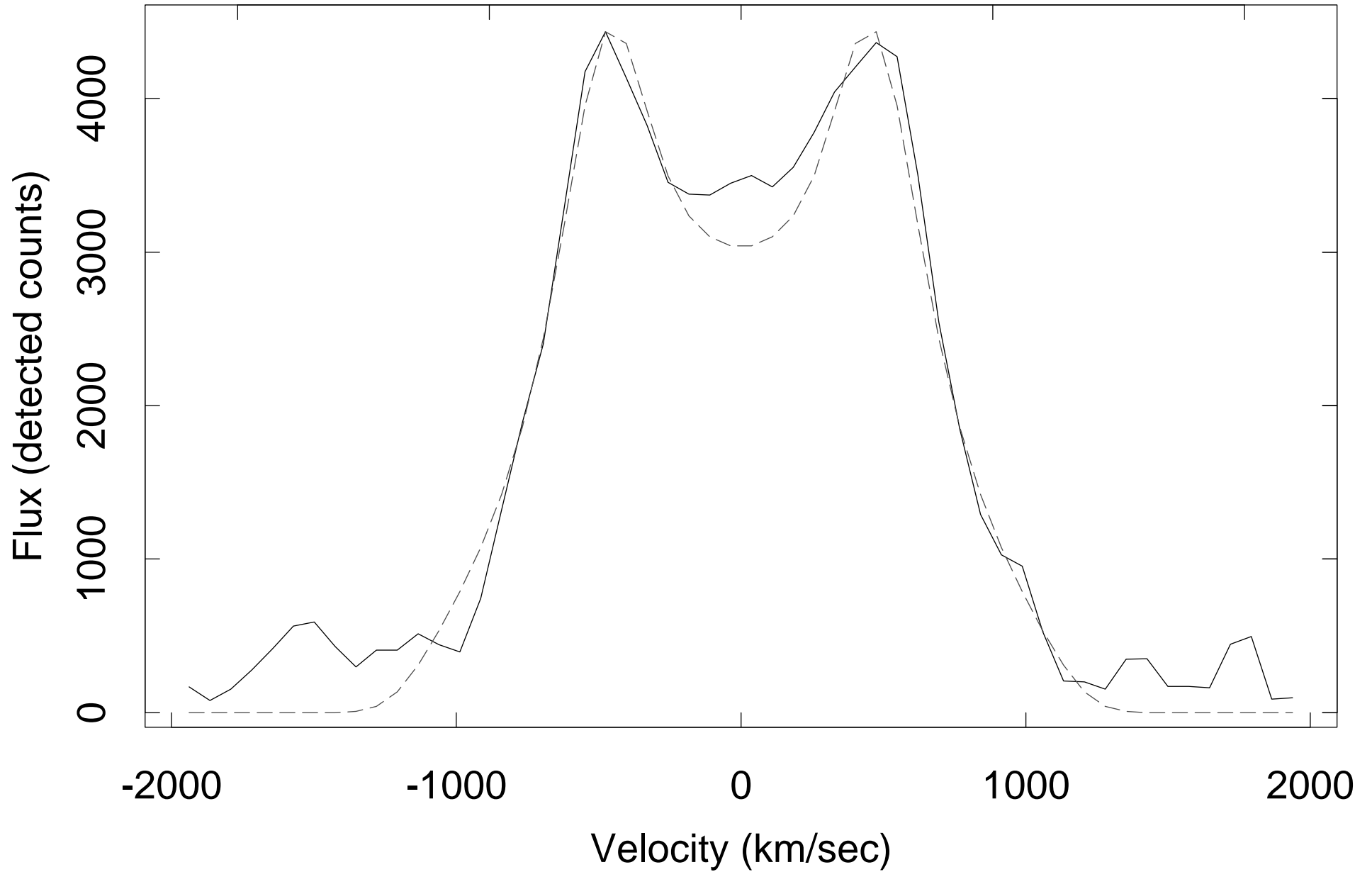
GRO J0422+32, Summed Oct 1993 Spectra

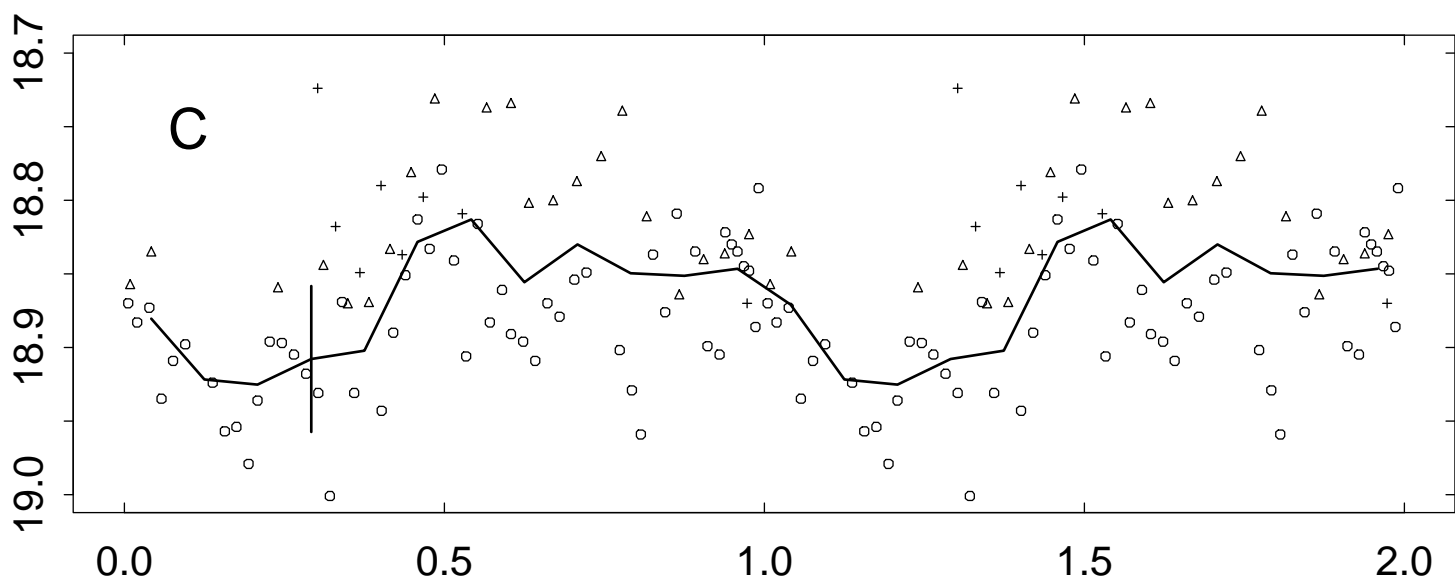
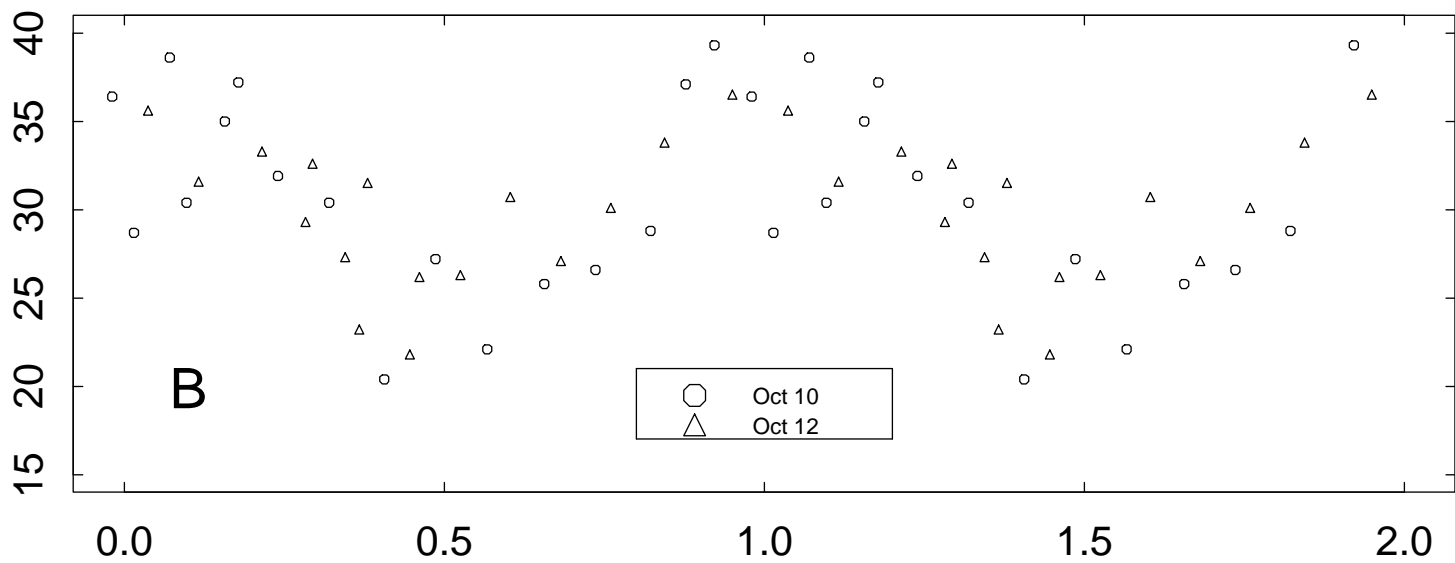
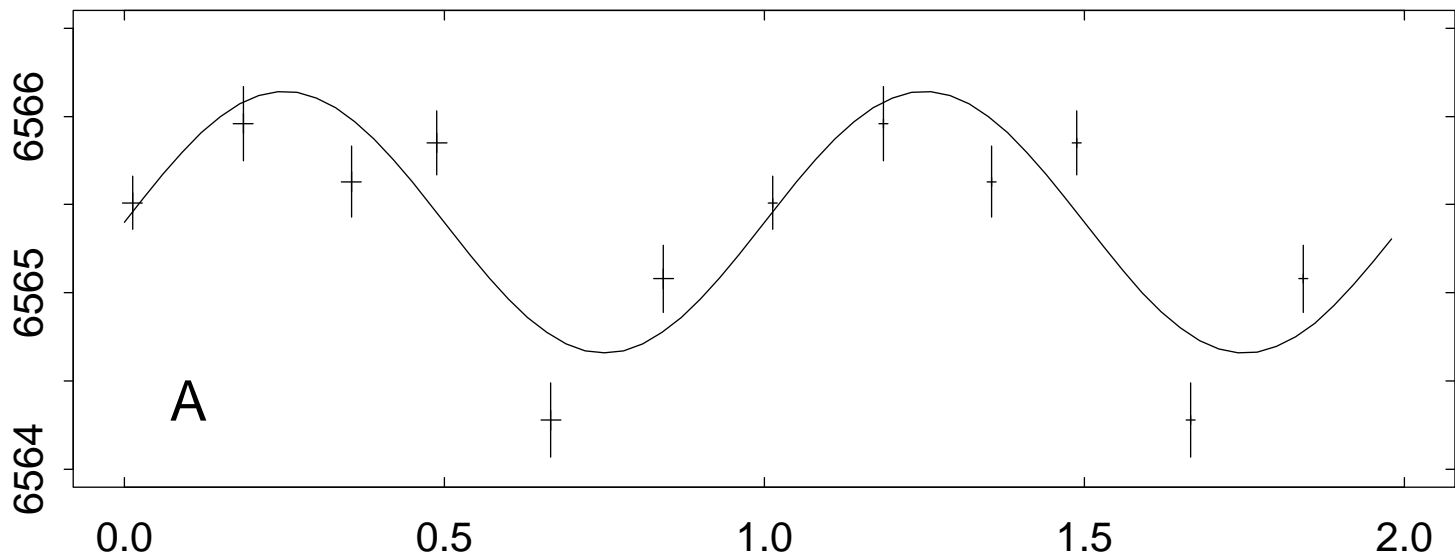


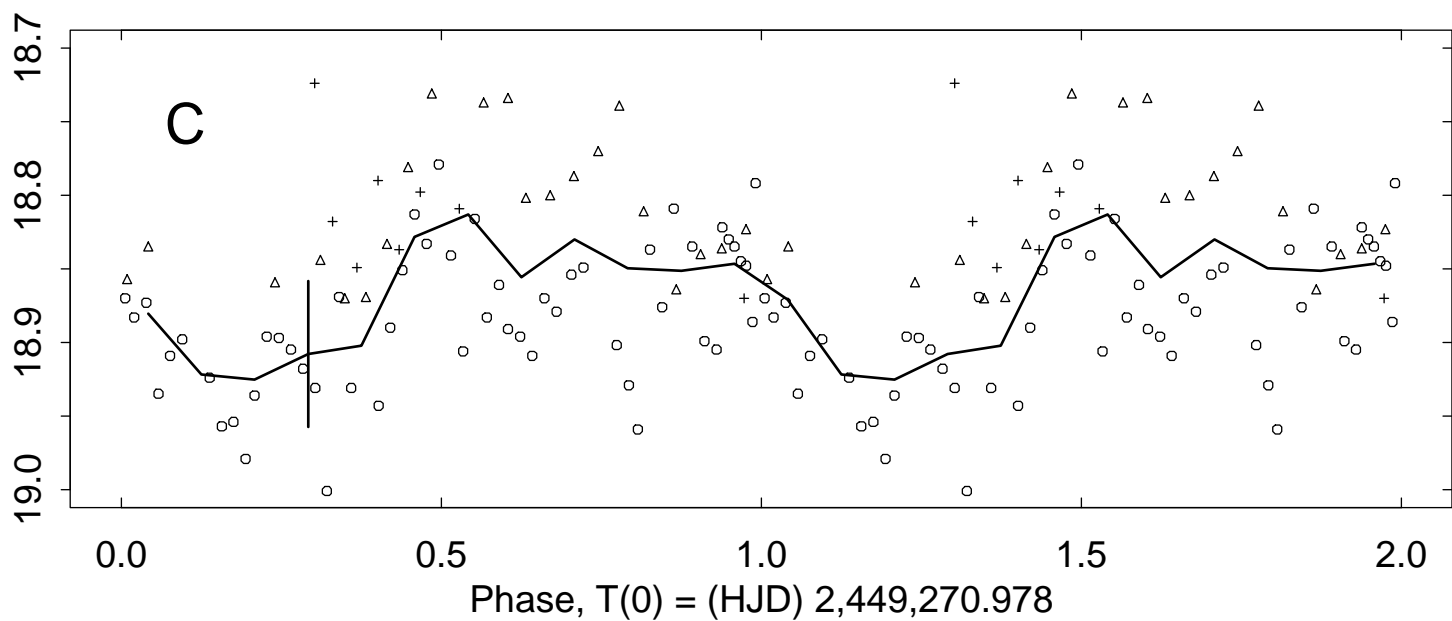
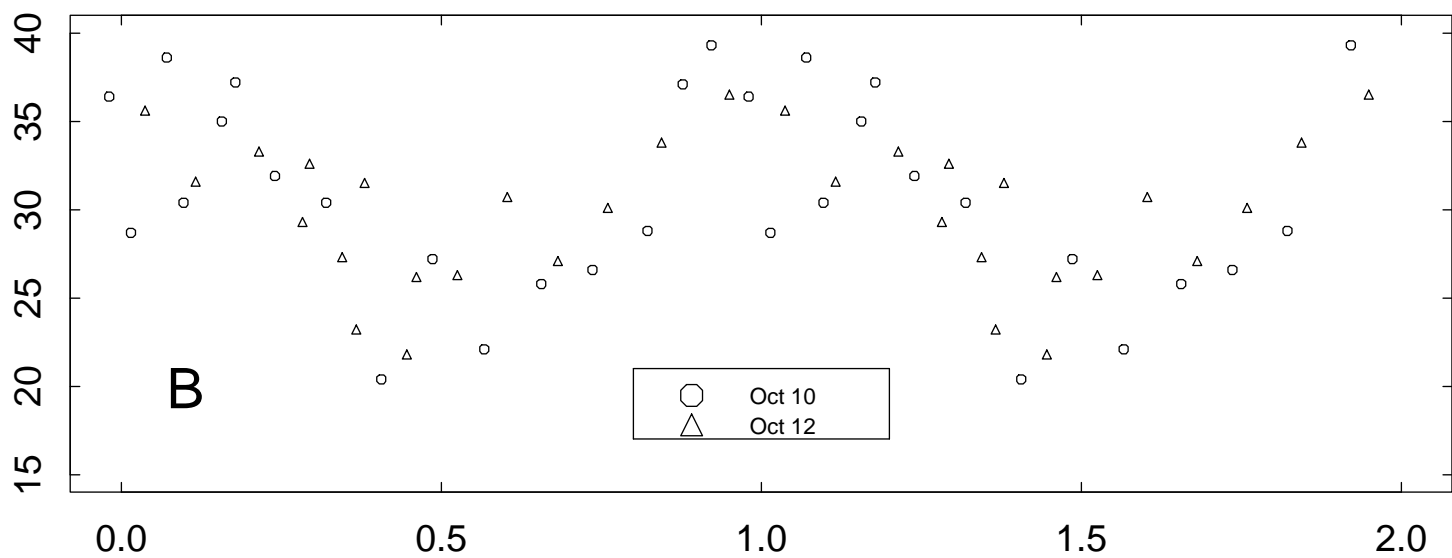
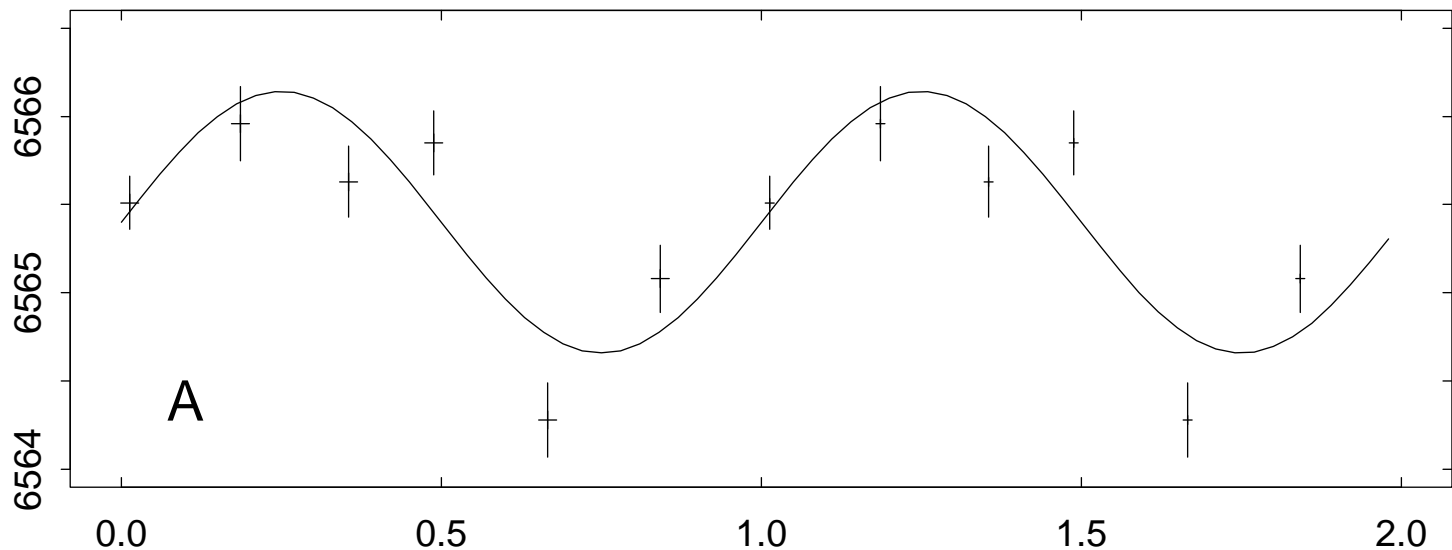
GRO J0422+32 and M3V

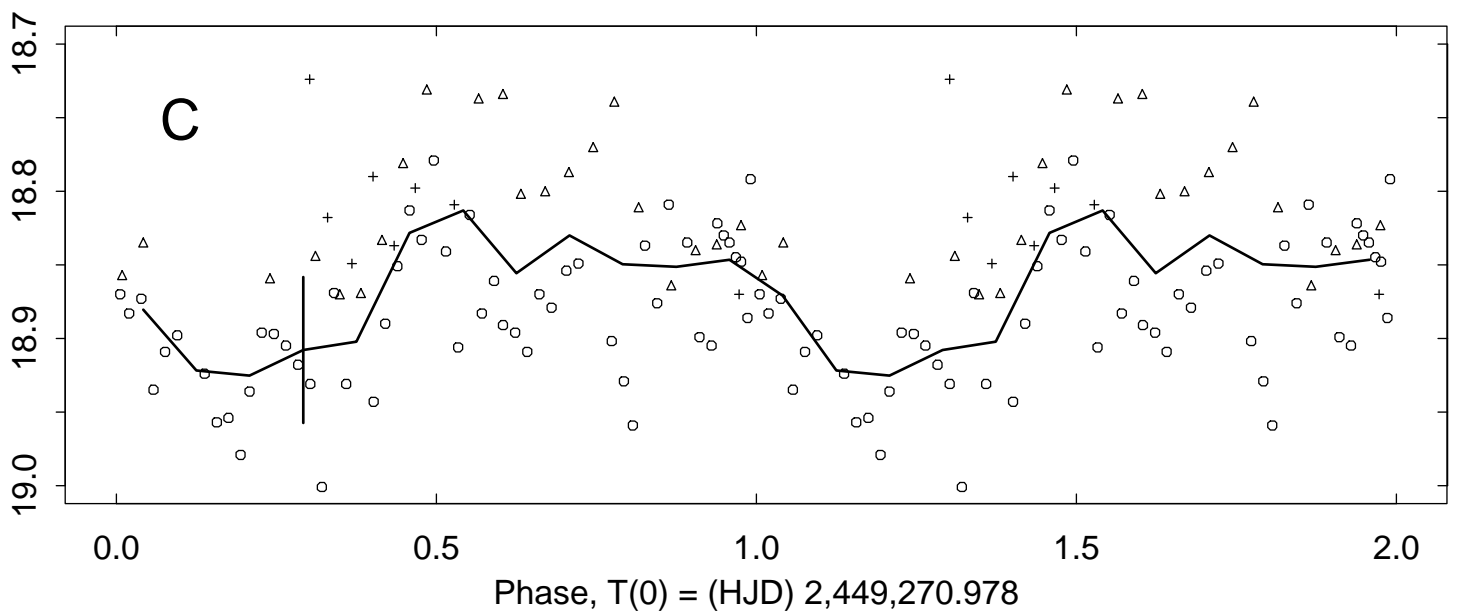
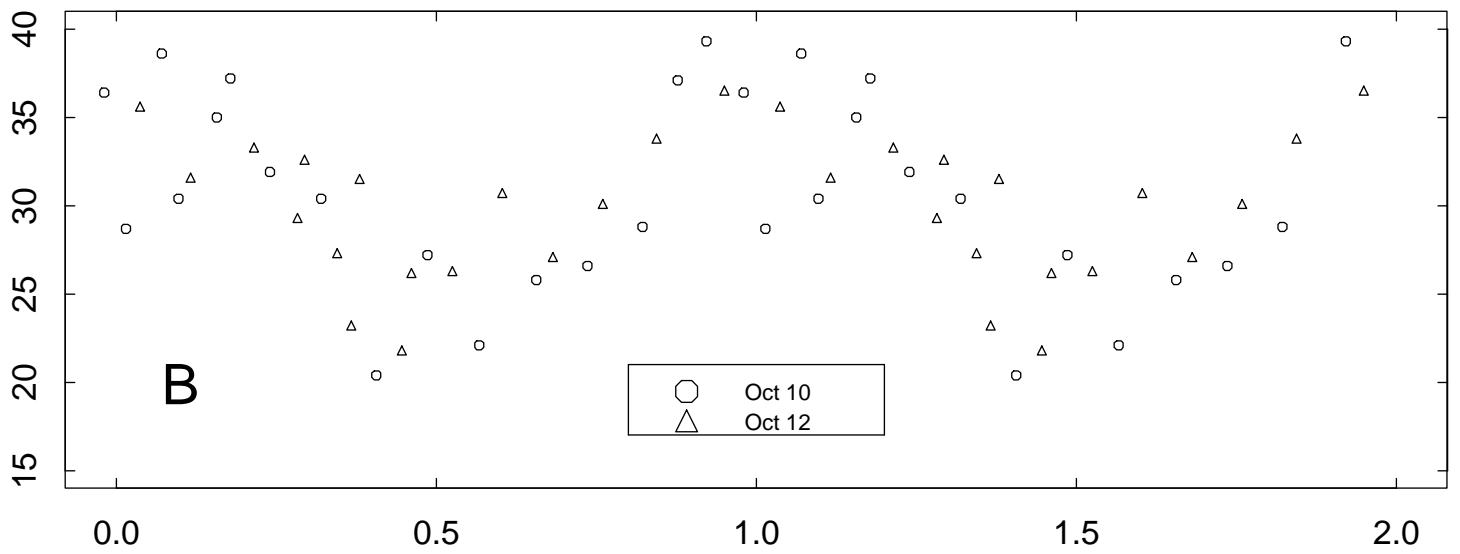
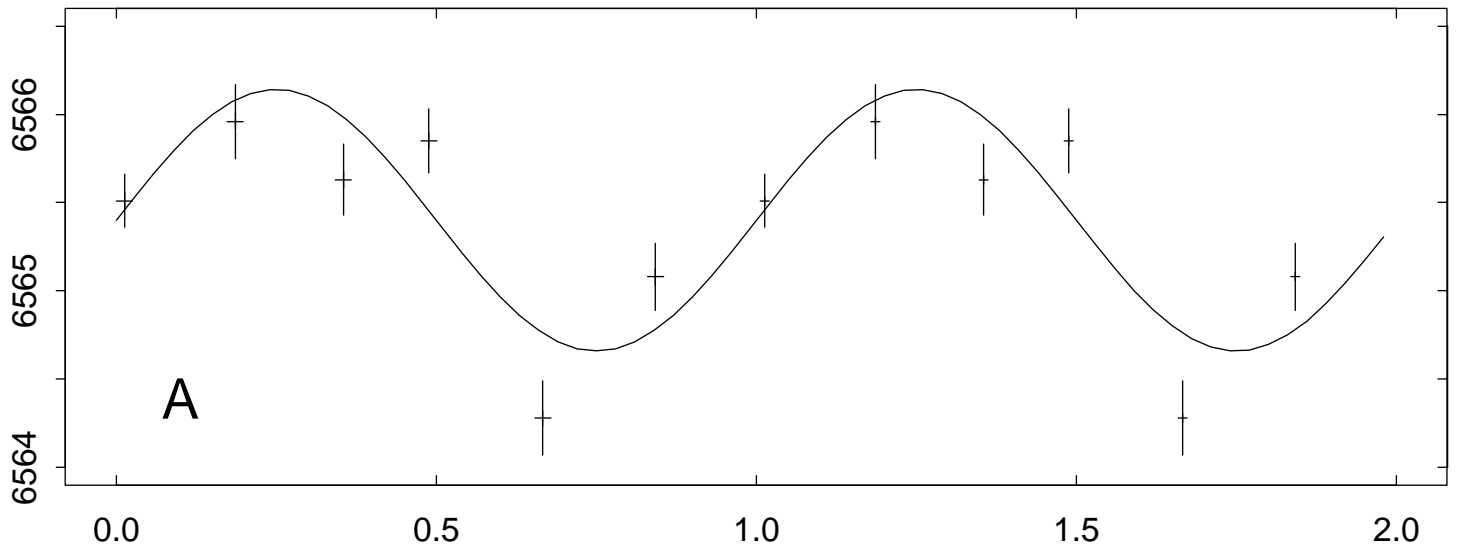


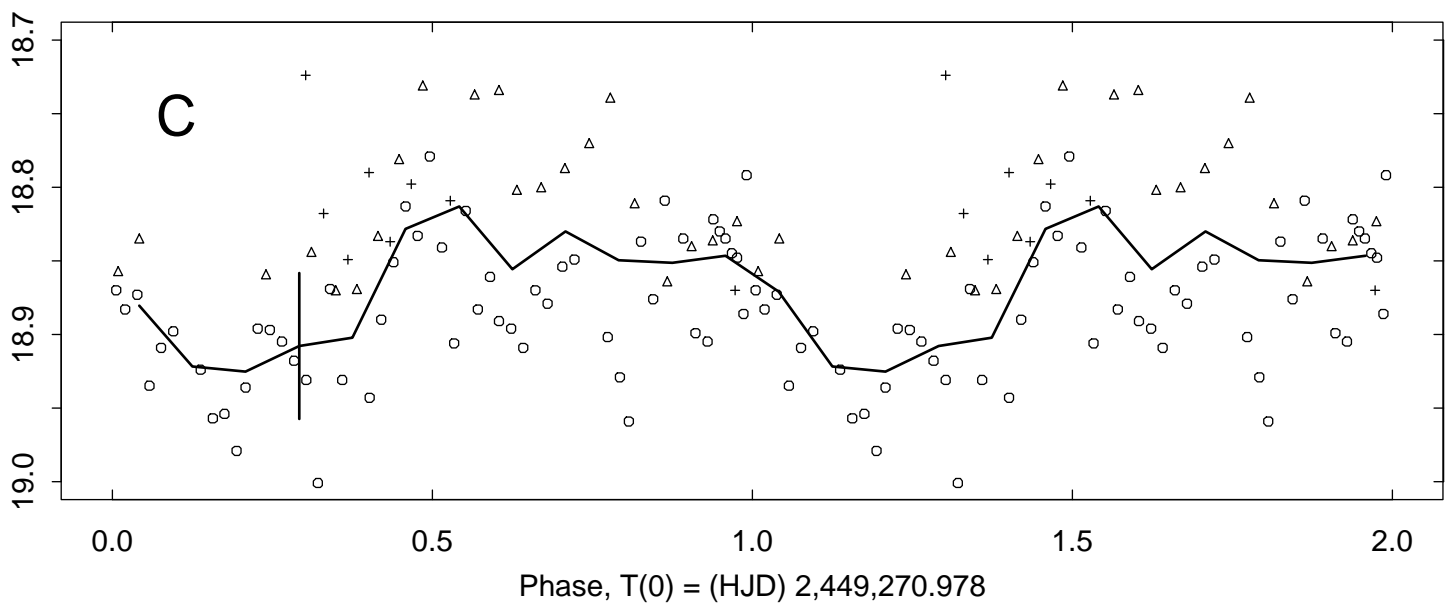
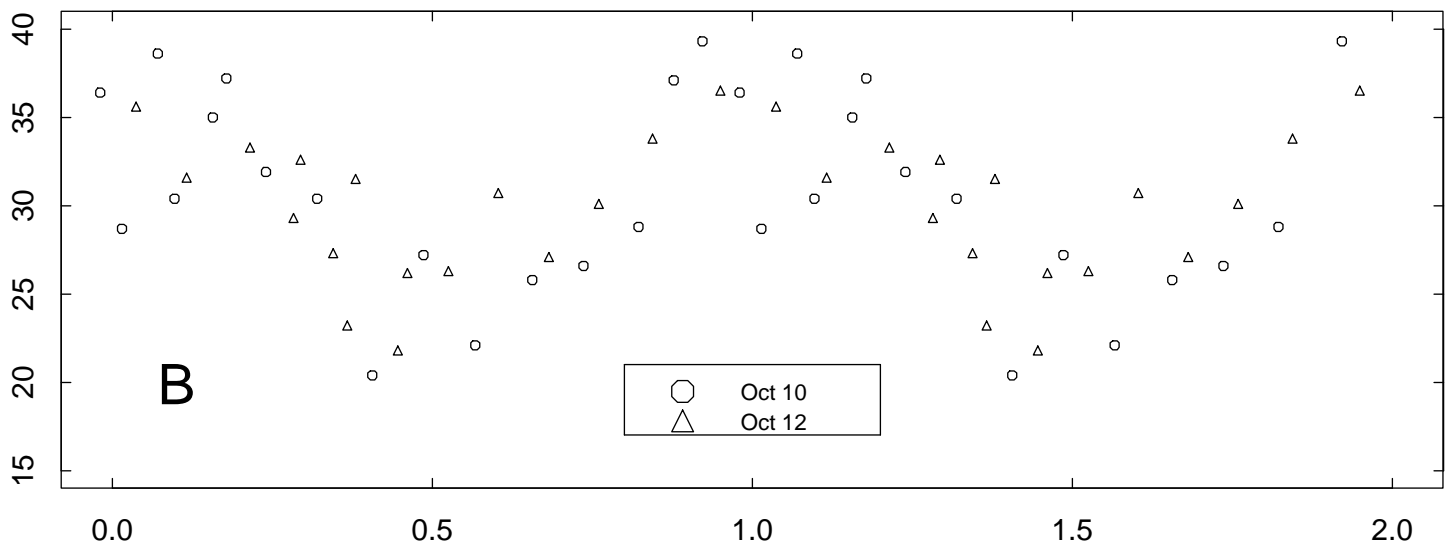
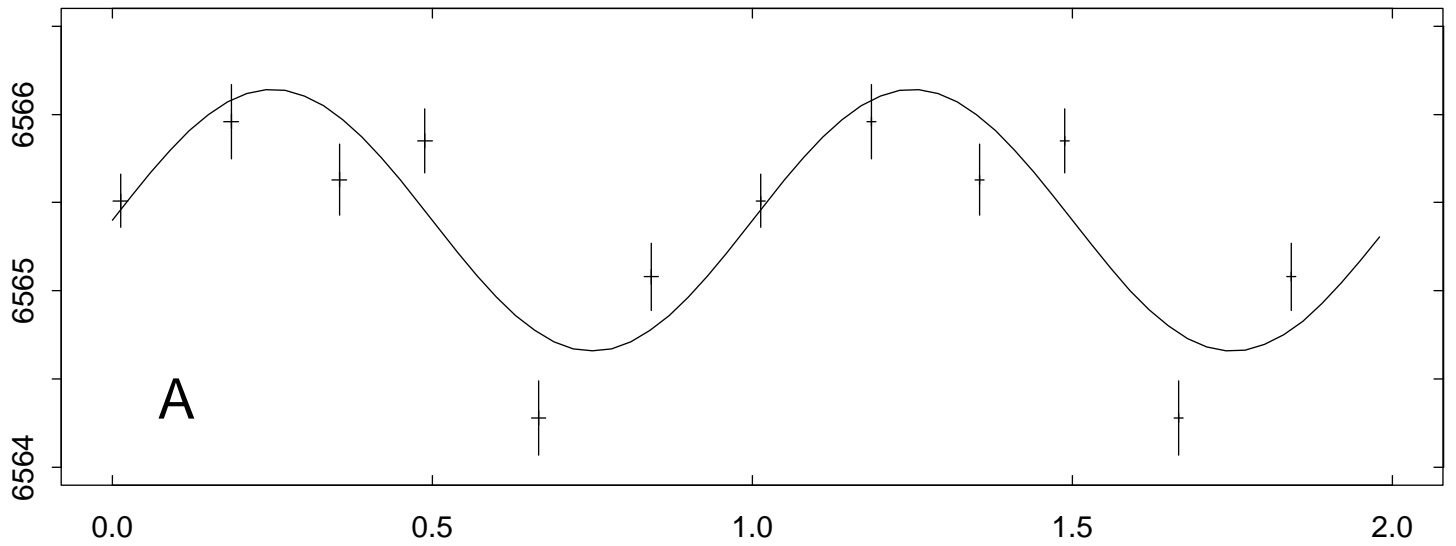
J0422+32 H-alpha Profile

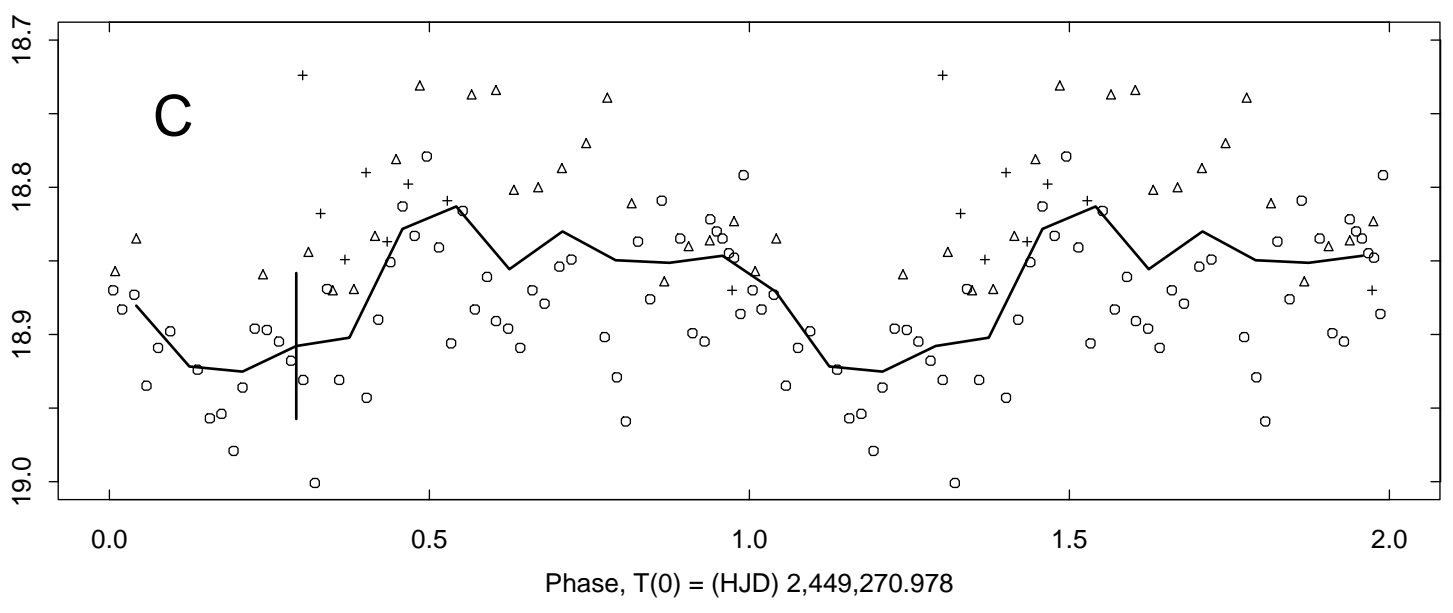
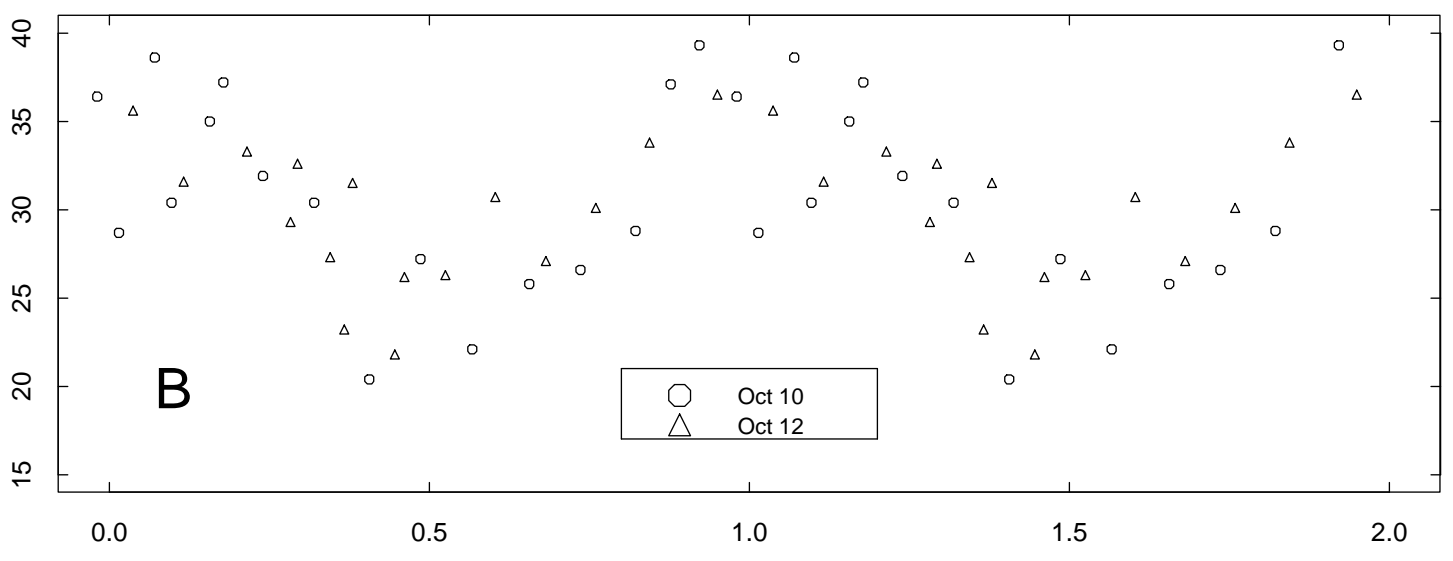
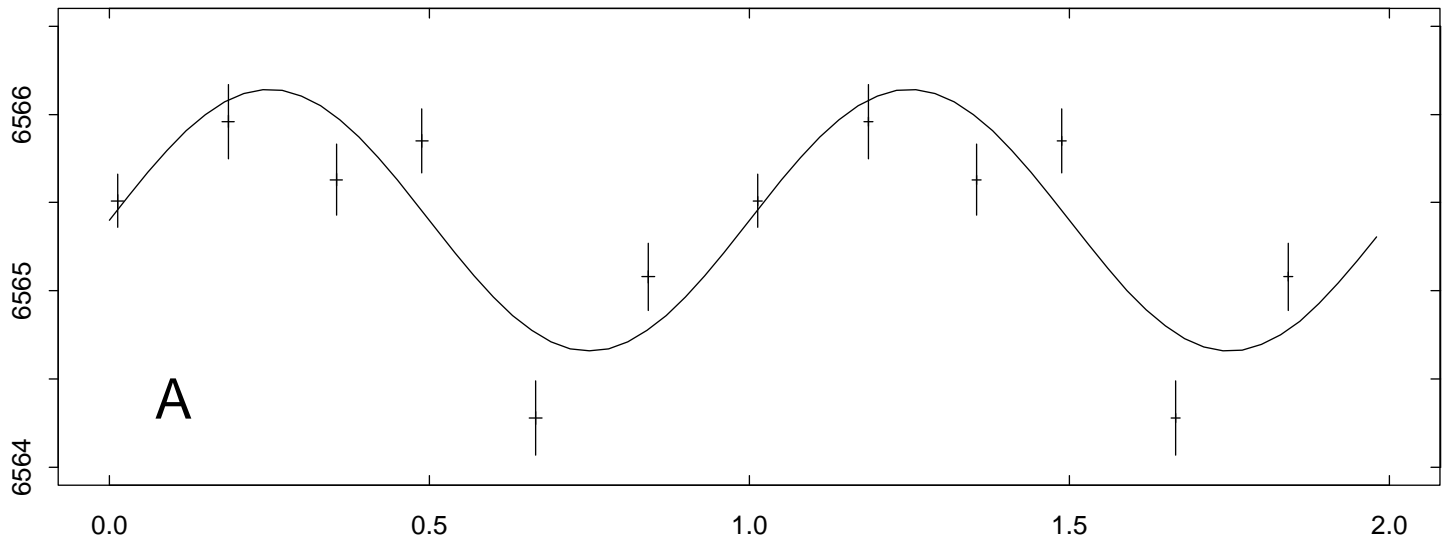


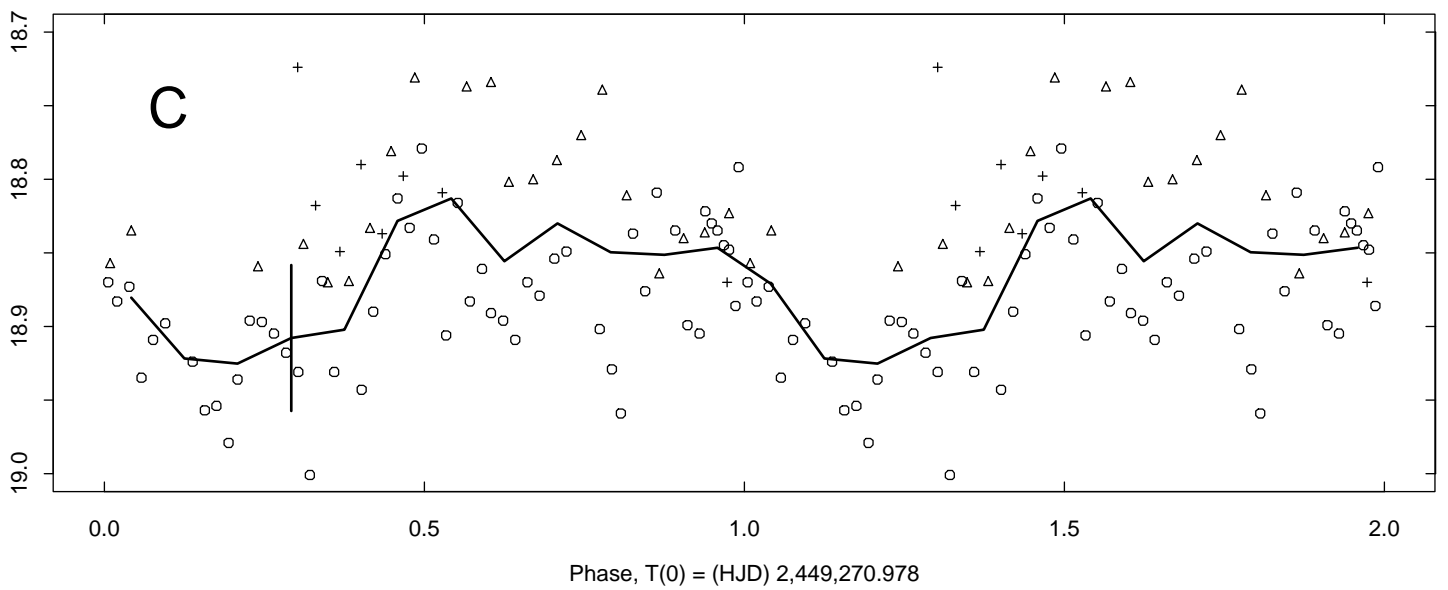
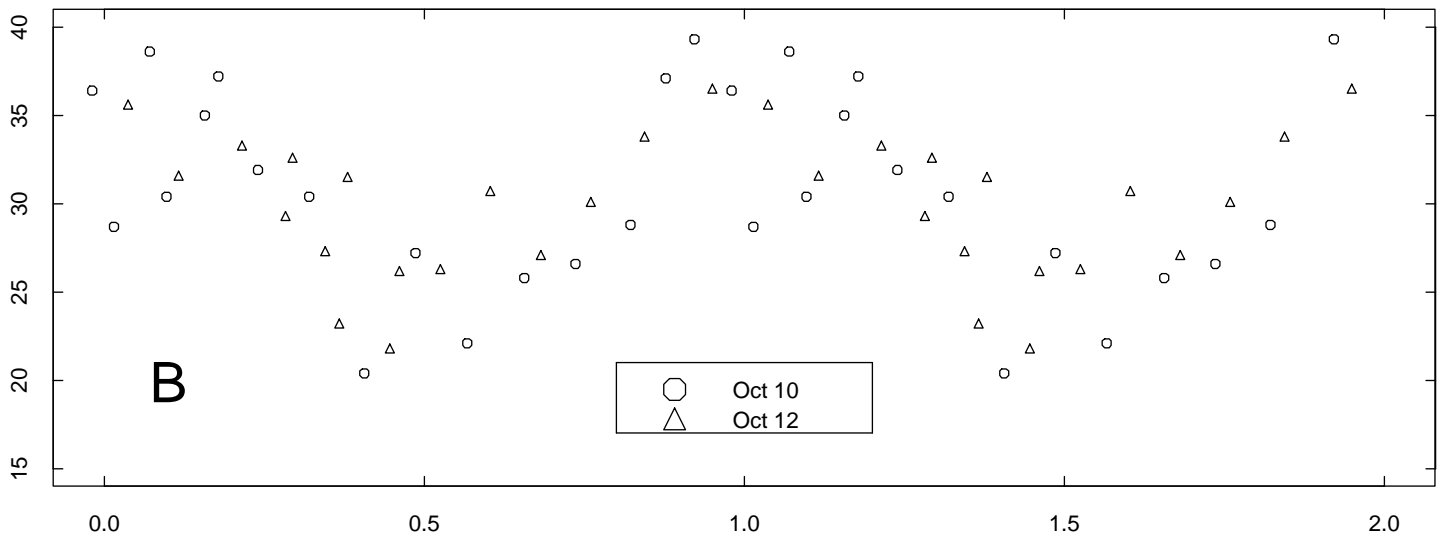
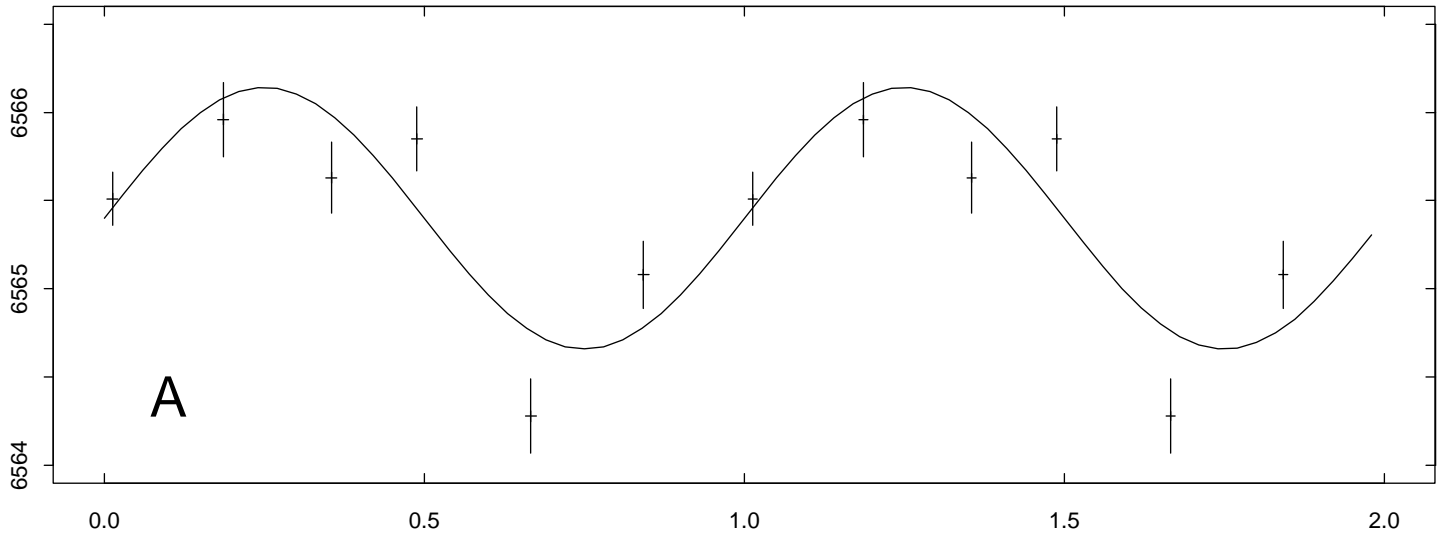












Phase, $T(0) = (\text{HJD}) 2,449,270.978$

